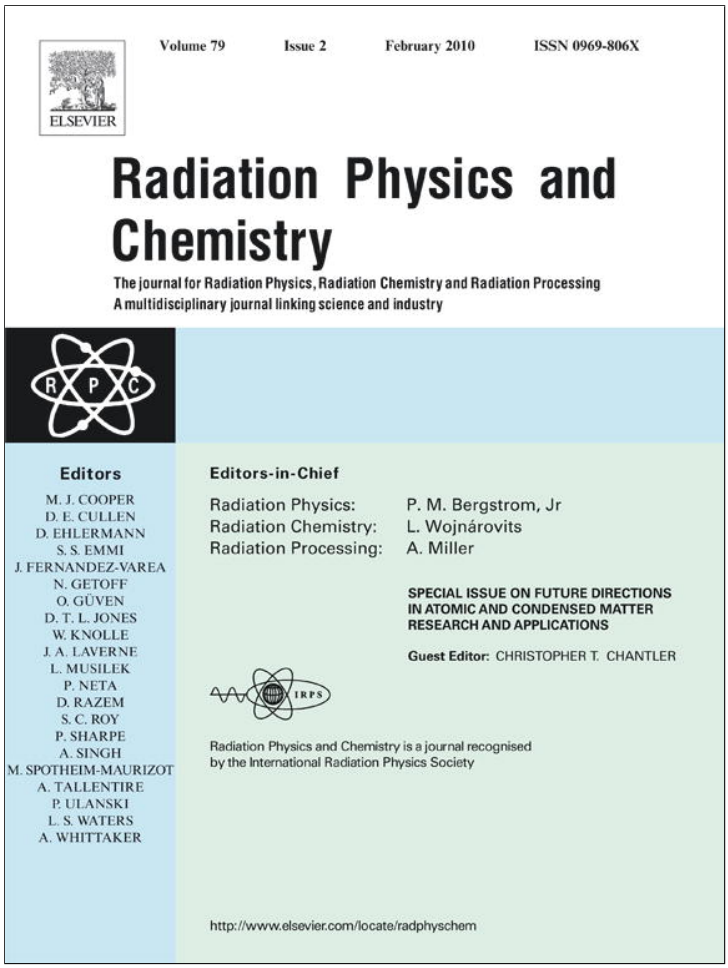

Radiation Physics and Chemistry 79 (2010) 124–131

Contents lists available at ScienceDirect

Radiation Physics and Chemistry

journal homepage: www.elsevier.com/locate/radphyschem

Compton scattering revisited

R.H. Pratt [a], L.A. LaJohn [a], V. Florescu [b], T. Surić [c,*], B.K. Chatterjee [d], S.C. Roy [d]

[a] Department of Physics and Astronomy, University of Pittsburgh, Pittsburgh, PA 15260, USA
[b] Centre for Advanced Quantum Physics, University of Bucharest, MG-11 Bucharest-Magurele, 077125 Magurele, Romania
[c] R. Bošković Institute, Bijenicka 54, 10000 Zagreb, Croatia
[d] Department of Physics, Bose Institute, Kolkata 700009, India

ARTICLE INFO

Article history:
Received 31 October 2008
Accepted 24 April 2009

PACS:
32.80.Aa

Keywords:
Compton scattering
Bound electrons
Inner shells
Compton profile
Impulse approximation
Relativistic impulse approximation
S-matrix

ABSTRACT

We review the standard theory of Compton scattering from bound electrons, and we describe recent findings that require modification of the usual understanding, noting the nature of consequences for experiment. The subject began with Compton and scattering from free electrons. Experiment actually involved bound electrons, and this was accommodated with the use of impulse approximation (IA), which described inelastic scattering from bound electrons in terms of scattering from free electrons. This was good for the Compton peak but failed for soft final photons. The standard theory was formalized by Eisenberger and Platzman (EP) [1970. Phys. Rev. A 2, 415], whose work also suggested why impulse approximation was better than one would expect, for doubly differential cross sections (DDCS), but not for triply differential cross sections (TDCS). A relativistic version of IA (RIA) was worked out by Ribberfors [1975. Phys. Rev. B 12, 2067]. And Surić et al. [1991. Phys. Rev. Lett. 67, 189] and Bergstrom et al. [1993. Phys. Rev. A 48, 1134] developed a full relativistic second order S-matrix treatment, not making impulse approximation, but within independent particle approximation (IPA).

Newer developments in the theory of Compton scattering include: (1) Demonstration that the EP estimates of the validity of IA are incorrect, although the qualitative conclusion remains unchanged; IA is not to be understood as the first term in a standard series expansion. (2) The greater validity of IA for DDCS than for the TDCS, which when integrated give DDCS, is related to the existence of a sum rule, only valid for DDCS. (3) The so-called "asymmetry" of a Compton profile is primarily to be understood as simply the shift of the peak position in the profile; symmetric and anti-symmetric deviations from a shifted Compton profile are very small, except for high Z inner shells where further $\vec{p}\cdot\vec{A}$ effects come into play. (4) Most relativistic effects, except at low energies, are to be understood in terms of simple kinematic modifications of nonrelativistic IA, plus using a relativistic charge density for high Z inner shell states; these shift the peak and change its height. However, for high Z, corrections to RIA persist in the peak region, even at extreme relativistic energies (correction of about 15% for $Z=92$).

1. Introduction

Since Compton's theoretical prediction (Compton, 1923a) of the increase in the wavelength (or shift in frequency) of X-rays due to scattering from a free electron at rest, and his experimental observation (Compton, 1923b) of the spectrum of scattered X-rays from electrons bound in a material, the process now named Compton scattering has been of great interest and the subject of intensive theoretical and experimental study. Today one of the main interests in the Compton scattering process is in fact in the modifications, caused by electron binding, of the results for scattering from a motionless free electron.

In Compton scattering of a photon with energy ω_i by a free electron at rest the scattered photon energy ω_f is determined by the scattering angle θ (this is the angle between the direction of incident photon momentum $\vec{k}_i$ and the outgoing photon momentum $\vec{k}_f$),

$$\omega_f = \omega_C = \frac{\omega_i}{1+\frac{\omega_i}{m}(1-\cos\theta)}, \tag{1}$$

as was predicted by Compton (1923a), by applying relativistic kinematics for X-ray quanta and electrons (Compton used wavelength rather than frequency in his discussions). Eq. (1) means that the spectrum of photons scattered from an electron at rest, for a fixed scattering angle θ, is a single line at frequency ω_C. The main purpose of the experiment performed by Compton

* Corresponding author. Tel.: +385 1 4571 302; fax: +385 1 4680 239.
E-mail addresses: rpratt@pitt.edu (R.H. Pratt), lal18@pitt.edu (L.A. LaJohn), flor@barutu.fizica.unibuc.ro (V. Florescu), suric@irb.hr (T. Surić), barun_k_chatterjee@yahoo.com (B.K. Chatterjee), suprakash.roy@gmail.com (S.C. Roy).
URL: http://stribor.phyast.pitt.edu/ (R.H. Pratt).

0969-806X/$ - see front matter © 2009 Elsevier Ltd. All rights reserved.
doi:10.1016/j.radphyschem.2009.04.035

(1923b) was to determine the frequency shift $(\omega_i - \omega_C)$. [The qualitative existence of a shift had earlier been reported by Gray (1920).] The experiment was performed by scattering molybdenum Kα lines from graphite at several angles. Within the experimental error, Compton demonstrated the validity of equation (1). (Due to binding, there is, however, in fact an additional shift.) In addition to the shifted line (inelastic photon scattering) Compton observed also an unmodified scattered photon line (elastic photon scattering).

Insufficient resolution of his apparatus did not allow Compton to observe in detail the actual modification of the modified spectral line due to binding of electrons in graphite. However, he noted that "There is a distinct difference between the widths of the unmodified and modified line". Later it became clearer that this difference in width is due to the binding effects, and that the modifications can provide information about the structure of the scatterer. This finding motivated further investigation of the Compton scattering process, going beyond the free electron case.

In the case of Compton scattering from free electron at rest the doubly differential cross section (DDCS) is determined by the Klein and Nishina (1929) formula

$$\frac{d^2\sigma}{d\Omega_f\, d\omega_f} = \frac{r_0^2}{4}\left(\frac{\omega_f}{\omega_i}\right)^2\left[\frac{\omega_f}{\omega_i} + \frac{\omega_i}{\omega_f} + 4(\vec{\varepsilon}_i\cdot\vec{\varepsilon}_f)^2 - 2\right]\delta(\omega_f - \omega_C), \tag{2}$$

where $\vec{\varepsilon}_i$ and $\vec{\varepsilon}_f$ are photon polarizations and r_0 is classical electron radius.

The Klein–Nishina formula is obtained using a full relativistic treatment both for the electron and for the photon–electron interaction (the photon is relativistic at all energies). However, one may also use a nonrelativistic treatment, in which case the γ–electron interaction is given by the A^2 term (the contribution of the $\vec{p}\cdot\vec{A}$ term vanishes for free electrons), and one obtains the Thomson DDCS

$$\left(\frac{d^2\sigma}{d\Omega_f\, d\omega_f}\right)_{Th} = r_0^2(\vec{\varepsilon}_i\cdot\vec{\varepsilon}_f)^2\left(\frac{\omega_f}{\omega_i}\right)^2\delta(\omega_f - \omega_C^{NR}), \tag{3}$$

where ω_C^{NR} is the nonrelativistic version of Eq. (1), obtained using nonrelativistic kinematics for the electron, which is close to ω_C up to relatively high energies, i.e. $\omega_C \simeq \omega_C^{NR} + O(\omega_i^4/m^3)$.

As already noted, for free electrons at rest, for each scattering angle there is just one scattering line at the position of ω_C and the strength of the line is given by Eq. (2). (There is no "unmodified line" in scattering from free electrons.) The appearance of the modified line, as well as its strength, in the Compton experiment was further studied after the Compton discovery. We know now that the spectrum (DDCS for a fixed angle) of photons scattered from a bound electron is not a single line but is continuous with, generally, three important features. This is schematically illustrated in Fig. 1, showing DDCS for scattering from an electron in the L-shell of an atom. The features are: infrared rise (the DDCS diverges for $\omega_f \to 0$), a resonant behavior near characteristic X-ray energies (if the ultimately ejected electron is not from the K-shell) and a relatively broad Compton peak in the vicinity of ω_C (if such region for ω_f is kinematically allowed), if ejecting an inner shell electron.

The feature of DDCS which Compton observed in his experiment, which is the most intensively studied feature and which is also the main subject of this paper, is the peak region. Here we will concentrate on scattering from inner shells, primarily discussing K-shell scattering (in which there are no resonant contributions). In our discussion we will also deal with the infrared region, in particular when dealing with high Z atoms. It is interesting to mention that the infrared rise of the DDCS of Compton scattering at low final photon energies has not been observed yet, despite several attempts.

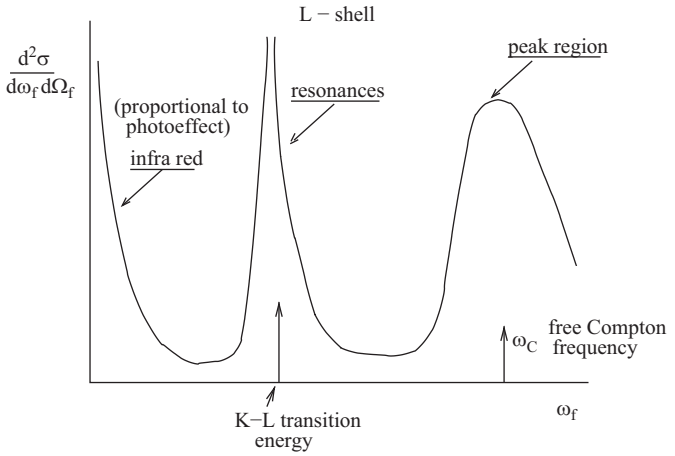

Fig. 1. Schematic illustration (not to scale) at fixed angle of the three main features of the doubly differential cross section: infrared rise, resonances at the characteristic X-ray energies, and a Compton peak in the vicinity of the Compton frequency ω_C.

In Section 2 we will present the idea of impulse approximation (IA), which was important in understanding the modifications of the DDCS in the Compton peak region due to binding effects. At the same time IA provided a very simple connection between the DDCS (observable) and the electronic structure in which the electron is bound. We discuss the early development of this idea in photon–atom scattering (it was also developed in nuclear particle scattering). In Section 3 we discuss the development of other approaches, which are more exact but also more complex, and which have generally also been restricted to treatments of the Compton process within independent particle approximation (IPA). These approaches include nonrelativistic A^2 approximation, the inclusion of nonrelativistic $\vec{p}\cdot\vec{A}$ terms, and also a full relativistic S-matrix approach. These approaches are important for more completely understanding all features of the Compton spectrum, but also for better understanding the validity of IA in the peak region. In Section 4 we describe some more recent results in the study of Compton scattering, which lead to a better understanding of IA and the Compton process, in wide ranges of energies and nuclear charge Z, including the ultrarelativistic regime. Much of the discussion is based on scattering from a Coulomb K-shell electron, which can be used to illustrate more general ideas, for simplicity and to take advantage of available analytical results. In Section 5 we summarize the situation.

2. Early work and the idea of IA

Early understanding of the broadening of the Compton line due to binding effects is largely connected with impulse approximation (IA). In IA, scattering from bound electrons is described as scattering from a momentum distribution $\rho(\vec{p})$ of free electrons. The distribution is determined by the electron wave function, i.e. $\rho(\vec{p}) = |\Psi(\vec{p})|^2$, where $\Psi(\vec{p})$ is the Fourier transform of the coordinate space electron wave function. In IA, the broadening of the Compton line, for scattering of photons from bound electrons, is therefore understood as due to a Doppler effect, when the photon is scattered from electrons with different velocities, whose distribution is given by $\rho(\vec{p})$. Note that in this picture the initial electron energy is not the binding energy E_B, but instead it is the energy of a free electron with momentum $\vec{p}$, for each choice of $\vec{p}$ in the distribution. In nonrelativistic quantum mechanics IA gives for the DDCS

$$\left(\frac{d^2\sigma}{d\omega_f\, d\Omega_f}\right)_{IA} = \left(\frac{d\sigma}{d\Omega_f}\right)_{Th}\frac{\omega_i}{\omega_f}J^{IA}(p_z), \tag{4}$$

where $(d\sigma/d\Omega_f)_{Th}$ is the Thomson singly differential cross section [Eq. (3) integrated over ω_f],

$$J^{IA}(p_z) = \int_{p_z}^{\infty} \rho(p) p\, dp, \tag{5}$$

for spherically symmetric charge distributions $\rho(p)$,

$$p_z = \frac{k}{2} - \frac{m(\omega_i - \omega_f)}{k}, \tag{6}$$

$\omega = \omega_i - \omega_f$ and $\vec{k} = \vec{k}_f - \vec{k}_i$ is the photon momentum transfer ($k = |\vec{k}|$).

This IA approach to Compton scattering from the quantum mechanical charge distribution of bound electrons was made by DuMond (1929) in his experimental and theoretical work in which scattering of photons from solids was studied. In his words "The diffusive structure of the Compton line is here attributed to a broadening caused by the velocity distribution of the scattering electrons in the solid scatterer analogous to a Doppler broadening and a relation between line structure and velocity distribution is derived." With this approach DuMond was able to distinguish between different theoretical predictions for the electron velocity distribution in metallic beryllium. [DuMond (1929) credits the IA approach to Jauncey (1925), who computed line structures using electrons in Kepler orbitals of the "old" quantum mechanics.]

DuMond justified his approach in comparing it with the quantum mechanical calculations of Wentzel (1927), who obtained the same results for the width of the Compton peak. DuMond (1933) argues that "when the binding energy of the electron is small compared to the recoil energy" then the IA "furnishes a valid method of studying the distribution of linear momentum in atoms". This would imply that $(a/k)^2 \ll 1$ is required for IA to be valid (since recoil momentum is roughly equal to k). We find that this criteria of validity of IA for DDCS, as we discuss in Sections 3 and 4, is too strong (although the DuMond criterion is valid for the triply differential cross section, when the direction of recoiled electron is observed, i.e. for the fundamental matrix element).

DuMond's work is the beginning of the use of Compton scattering as a tool for studying electronic structure, in which IA provides the connection between the observable (DDCS) and the structure [$\rho(p)$]. The widespread use of the method and consequent renewed interest in Compton scattering during 1960s for studying electronic structure (Cooper et al., 1965) motivated further studies of IA, and its extension to the relativistic region. In addition, development of experimental methods in the 1970s allowed to distinguish contributions to DDCS Compton scattering from inner shells (Prasad et al., 1977), which motivated development of more exact approaches, including relativistic approaches.

IA was shown to be useful not only for the description of inelastic photon scattering but also for the description of particle collisions. Fermi (1936) was first to suggest the use of IA for the description of neutron scattering from bound hydrogen atoms. This approach was further developed by Chew (1950), Chew and Wick (1952) and others, while justification of IA in particle collisions, with criteria of validity was given by Wick (1954).

Further study of the Compton scattering process developed generally in two directions: (1) the study of Compton scattering from weakly bound valence electrons and bands for determining structure and magnetic properties of materials, for which only the peak region of the DDCS spectrum is important, and for which the IA is generally adequate (although, generally, small discrepancies are observed), and (2) the study of Compton scattering from inner shells (strongly bound electrons) in which the binding effects are strong and IA is generally inadequate, even for the peak region. A more detailed history of developments can be found in Cooper (1985), Kane (1992), and Bergstrom and Pratt (1997). Our discussion here will primarily focus on this second direction of study.

In work in the first direction of study, the results of measurements of DDCS are expressed often in terms of the so-called Compton profile. It has been common to distinguish DDCS from Compton profile by extracting the kinematical factor. There are two kinematical factors, the nonrelativistic and the relativistic one. There are still two possibilities—Compton profile can be defined from DDCS by removing this kinematical factor or it can be defined from impulsive results. One finds different uses in the literature, which is also reflected in this manuscript.

In the nonrelativistic domain two definitions of Compton profile are in use. They are often taken as identical which, however, is true only in the nonrelativistic IA. The first definition (for spherically symmetric charge distributions) is given by Eq. (5) (here it is a theoretical quantity). However, in observations one measures DDCS. In the nonrelativistic region, when unpolarized photons are used [summation over the polarization directions $\vec{\varepsilon}_f$ and averaging over $\vec{\varepsilon}_f$ is done in Eq. (3)], the Compton profile may be defined as (the experimental quantity)

$$J(p_z, k) = \frac{\left(\dfrac{d^2\sigma}{d\omega_f\, d\Omega_f}\right)}{\dfrac{1}{2} r_0^2 (1 + \cos^2(\theta)) \dfrac{m}{k} \dfrac{\omega_f}{\omega_i}}. \tag{7}$$

The Compton profile, so defined, is generally taken to be a function of two variables, which are usually taken to be p_z given by Eq. (6), and photon momentum transfer k. (This is valid within A^2 approximation.) Only in nonrelativistic IA is it a function of a single variable p_z and equivalent to the definition equation (5). In spherically symmetric situations, the IA Compton profile is given by Eq. (5), which we may take as its definition, with a relativistic generalization to be noted below.

3. Development of theory of Compton scattering from bound electrons

In nonrelativistic quantum mechanics the interaction between the electron and photon is described by the interaction Hamiltonian

$$H_{int} = \frac{e^2}{2m} A^2 - \frac{e}{m} \vec{p} \cdot \vec{A}, \tag{8}$$

where e is the electron charge. Most early development of the theory of Compton scattering was based on this nonrelativistic e–γ interaction, but restricted to just the A^2 term, which gives the dominant contribution to the peak region. (For free electrons the A^2 term is the only term that contributes.)

The description of the DDCS for Compton scattering from bound electrons can be traced back to Wentzel (1927), who used a full nonrelativistic quantum mechanical treatment, with the A^2 term of the e–γ interaction. Making some additional approximations he was able to reproduce the broadening of the free Compton line. Later, Schnaidt (1934) obtained the full Coulomb K-shell result within the A^2 approximation, while Bloch (1934) extended these calculations to L-shells. (These results contained some errors which were later corrected.) Schumacher et al. (1975) extended A^2 calculations to all Coulomb shells.

In the energy region in which Compton peak is not visible (small incident energies or forward angles), or for small scattered photon energies ($\omega_f \to 0$), the $\vec{p} \cdot \vec{A}$ term becomes dominant. The calculation of DDCS within $\vec{p} \cdot \vec{A}$ was done by Gavrila (1972) for the Coulomb K-shell, including the infrared rise feature of the DDCS, and by Costescu and Gavrila (1973) and Gavrila and

Tugulea (1975) for the Coulomb L-shell, thereby including the resonant feature of the DDCS.

A full relativistic treatment of DDCS using second order S-matrix theory within self-consistent screened IPA potentials was achieved by Surić et al. (1991) and Bergstrom et al. (1993). Within this treatment all the main features of the DDCS are included. An extension of this approach for describing the triply differential cross section (TDCS) was made by Kaliman et al. (1998). The S-matrix treatment is numerical and is limited to incident photon energies up to about 1 MeV. [There had been earlier attempts by Whittingham (1971), which encountered problems and also limited results of Wittwer (1972).] Very recently, also the ultrarelativistic result for the Coulomb K-shell became available (Florescu and Gavrila, 2003). All of these full quantum mechanical treatments have been limited to IPA descriptions of electron binding. They are very helpful in understanding many aspects and features of the Compton process. They are not expected to be adequate in resonance regions near the ionization thresholds.

In Compton scattering we still do not have precise criteria for the validity of IA, although we do have some understanding from the comparison with more exact approaches in IPA models [as done e.g. in Bloch and Mendelsohn (1974)]. Important contributions to the development and understanding of nonrelativistic IA can be found in the work of Platzman and Tzoar (1965) and Eisenberger and Platzman (1970), in which some derivation of the DuMond IA result was given. However, the criteria of validity of IA for DDCS derived by Eisenberger and Platzman (1970), that IA is valid for $(a/k)^4 \ll 1$, is not correct, as we discuss in the next section. We know that IA is fairly good even for $a/k \simeq 1$ for DDCS even though the expansion of the exact DDCS (Coulomb K-shell, for example) in powers of a/k is not convergent for $a/k = 1$. IA is not good for TDCS unless $a/k \ll 1$ (not considered by EP).

Relativistic IA (RIA) was developed by Ribberfors (1975), using the approach of DuMond, i.e the scattering of photons by bound electrons is viewed as scattering from a distribution of free electrons. However, unlike in the nonrelativistic IA in A^2 approximation, in RIA the DDCS, including the relativistic equivalents of $\vec{p}\cdot\vec{A}$ terms, does not factorize into a kinematical factor and a Compton profile, and so it does not provide a simple connection between the DDCS and $\rho(p)$. By making further approximations Ribberfors argued that this connection (factorization in terms of Compton profile) can be established with small errors or corrections. The justification of RIA can also be based on comparisons with full relativistic IPA calculations. The comparison shows (Surić, 1992; LaJohn, 2009) that at high photon energies RIA gives a good description of the peak region with some errors for high Z. The comparison of RIA with ultrarelativistic calculations (Florescu and Pratt, 2009) shows that for low Z this agreement is indeed very good, while for high Z disagreement up to about 15% for $Z = 92$ persists.

4. New developments

In this section we describe more recent results, which lead to a better understanding of IA and the Compton process in a wide range of energies and nuclear charge Z. We discuss also the ultrarelativistic region. Much of our discussion is based on scattering from a Coulomb K-shell electron, which provide a useful example. We discuss the validity of nonrelativistic IA for TDCS, the validity of IA as the leading order term in an a/k expansion of the exact DDCS, the so-called asymmetry of the Compton profile, and the relativistic behavior of the DDCS, including the ultrarelativistic limit.

4.1. Validity of nonrelativistic IA for TDCS

The IA, as defined by DuMond, can easily be applied to TDCS. For the Coulomb K-shell scattering, for which the momentum density is

$$\rho(p) = \frac{16a^5}{\pi(a^2+p^2)}, \tag{9}$$

the TDCS is

$$\left(\frac{d^3\sigma}{d\omega_f\, d\Omega_f\, d\Omega_e}\right)_{IA} = \frac{1}{2} r_0^2(1+\cos^2\theta)\frac{\omega_f}{\omega_i}\frac{16a^5}{\pi^2} \times \int \frac{p^2 dp}{(a^2+(\mathbf{k}-\mathbf{p})^2)^4}\delta\left(\frac{p^2}{2m} - \frac{(\mathbf{p}-\mathbf{k})^2}{2m} - \omega\right), \tag{10}$$

where $\omega = \omega_i - \omega_f$ and $d\Omega_e = \sin\beta\, d\beta\, d\Phi$. With the δ-function,

$$\delta\left(\frac{p^2}{2m} - \frac{(\mathbf{p}-\mathbf{k})^2}{2m} - \omega\right) = \delta\left(\frac{\mathbf{p}\cdot\mathbf{k}}{m} - \frac{k^2}{2m} - \omega\right), \tag{11}$$

one can perform the integration, since the angle β between $\mathbf{p}$ and $\mathbf{k}$ is fixed. Note that $\cos\beta$ must be positive, otherwise the δ-functions give zero result. Provided that $\cos\beta > 0$ one obtains

$$\left(\frac{d^3\sigma}{d\omega_f\, d\Omega_f\, d\Omega_e}\right)_{IA} = \frac{1}{2} r_0^2(1+\cos^2\theta)\frac{\omega_f}{\omega_i}\frac{16ma^5}{k\cos\beta\pi^2}\frac{p^2}{(a^2+(\mathbf{k}-\mathbf{p})^2)^4}, \tag{12}$$

where $p = p_z/\cos\beta$, with p_z defined as in Eq. (6).

This result we may compare with the full A^2 result for the K-shell TDCS (Eisenberger and Platzman, 1970 quoting Gummel and Lax, 1957)

$$\frac{d^3\sigma}{d\omega_f\, d\Omega_f\, d\Omega_e} = \frac{1}{2} r_0^2(1+\cos^2\theta)\frac{\omega_f}{\omega_i} m p_f |M_{fi}|^2, \tag{13}$$

where $p_f^2 = 2m(\omega - |E_b|)$, and

$$|M_{fi}|^2 = \frac{512\pi^2 a^6 e^{-(2a/p_f)Arccos\frac{k^2+a^2-p_f^2}{\sqrt{(k^2+a^2-p^2)^2+4a^2p_f^2}}}}{p_f(1-e^{-2\pi a/p_f})} \times \frac{(\vec{k}\cdot(\vec{k}-\vec{p}_f))^2 + \left(a\frac{\vec{p}_f\cdot\vec{k}}{p_f}\right)^2}{((k^2-p_f^2+a^2)^2+4p_f^2a^2)(a^2+(\vec{k}-\vec{p}_f)^2)^4}. \tag{14}$$

Note that the TDCS does not depend on the angle Φ.

In Figs. 2 and 3 we compare IA and full A^2 results for TDCS for Compton scattering of 10 keV photons from the Be K-shell as a function of the angle β. The outgoing photon energies are chosen from the vicinity of the Compton peak in DDCS at $\theta = 140^\circ$. Although $a/k = 0.54$ the disagreement between the IA and A^2 results is large in essentially all cases. From the comparison we may conclude that: (1) IA for TDCS is only valid at high energy, $a/k \ll 1$; (2) for a given $a/k \simeq 1$ IA is bad for TDCS for all angles β; (3) for the angles $\beta > 90^\circ$ IA predicts that TDCS vanishes, although TDCS is not negligible in this region for $a/k \simeq 1$.

However, integrating over β ($\sin\beta\, d\beta$) results in generally good DDCS. This cancellation of errors in TDCS to give a good DDCS presumably reflects the existence of a sum rule, as used by Eisenberger and Platzman (1970) when summing over all electron states in going from TDCS to DDCS.

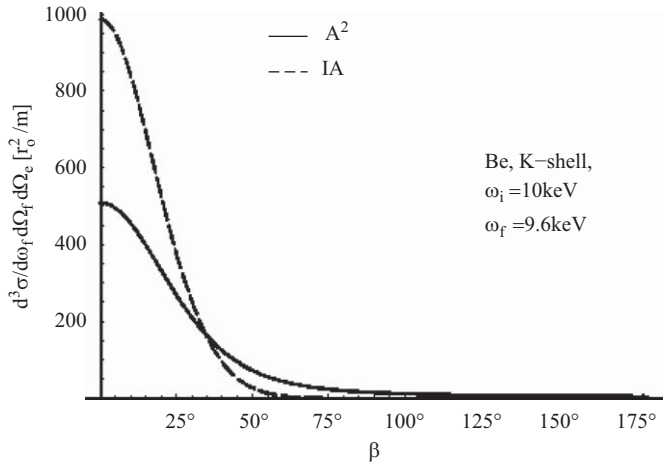

Fig. 2. TDCS for Compton scattering of 10 keV photons from the Be K-shell as a function of the angle β between the outgoing electron and the momentum transfer k. Outgoing photons have energy $\omega_f = 9.66$ keV and the photon scattering angle is $\theta = 140^\circ$, which corresponds to the peak region ($p_z = 0$). The solid line shows A^2 results and the dashed line shows IA results.

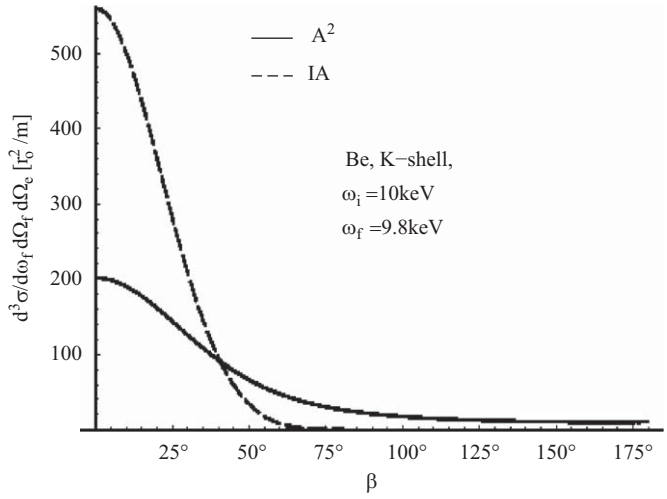

Fig. 3. The same as Fig. 2 except $\omega_f = 9.85$ ($p_z = 1.6$ a.u.).

4.2. Validity of nonrelativistic IA for DDCS: a/k expansion

The IA for DDCS is often viewed as the leading term in the a/k expansion of the exact result (Tavard et al., 1983; Holm and Ribberfors, 1989). For the hydrogen-like system in the A^2 approximation the DDCS is (Eisenberger and Platzman, 1970)

$$\frac{d^2\sigma}{d\omega_f\, d\Omega_f} = \frac{1}{2}(1+\cos^2\theta)\frac{\omega_f}{\omega_i}\,\frac{256k^2a^6\pi}{3} \times \frac{e^{-2a/p_f \mathrm{Arccos}\left(\frac{a^2+k^2-p_f^2}{\sqrt{(a^2+k^2-p_f^2)^2+4a^2p_f^2}}\right)}}{1-e^{-2\pi a/p_f}} \times \frac{a^2+3k^2+p_f^2}{((a^2+k^2-p_f^2)^2+4a^2p_f^2))^3}. \quad (15)$$

By using Eq. (7) we obtain the exact analytic expression for the K-shell Compton profile, so defined,

$$J(p_z,k) = B\left(\frac{p_z}{a},\frac{a}{k}\right)J^{IA}(p_z), \quad (16)$$

where

$$J^{IA}(p_z) = \frac{8a^5}{3\pi(a^2+p_z^2)^3}, \quad (17)$$

and

$$B\left(\frac{p_z}{a},\frac{a}{k}\right) \equiv B(x,y) = 2\pi y\left(1-\frac{x\cdot y}{2}\right)\frac{e^{-2y\frac{\mathrm{Arccos}\left(-\frac{x+y}{\sqrt{1+x^2}}\right)}{\sqrt{1-2xy-y^2}}}}{1-e^{-\frac{2\pi y}{\sqrt{1-2xy-y^2}}}} \quad (18)$$

is an asymmetric function in p_z.

By expanding the function $B(p_z/a, a/k)$ in the vicinity of the Compton peak we may analyze the convergence of the a/k expansion. Expanding around $p_z/a = 0$ (vicinity of the peak) and $a/k = 0$ we obtain

$$B\left(\frac{p_z}{a},\frac{a}{k}\right) = 1+\frac{9-\pi^2}{6}\left(\frac{a}{k}\right)^2+\frac{795-150\pi^2+7\pi^4}{360}\left(\frac{a}{k}\right)^4 + O\left(\left(\frac{a}{k}\right)^6\right)+\frac{1}{2}\left(1+\frac{5(9-\pi^2)}{6}\left(\frac{a}{k}\right)^2 + \frac{795-150\pi^2+7\pi^4}{40}\left(\frac{a}{k}\right)^4+O\left(\left(\frac{a}{k}\right)^6\right)\right)\frac{a}{k}\frac{p_z}{a} \simeq 1 - 0.14\left(\frac{a}{k}\right)^2 - 0.01\left(\frac{a}{k}\right)^4 + 0.001\left(\frac{a}{k}\right)^6 + \left(0.5-0.36\left(\frac{a}{k}\right)^2 - 0.05\left(\frac{a}{k}\right)^4 + 0.005\left(\frac{a}{k}\right)^6\right)\frac{a}{k}\frac{p_z}{a}+\cdots. \quad (19)$$

Looking at higher order terms, the convergence of a/k expansion is poor unless a/k is small. But the coefficients of all terms in the expansion are small (in particular for p_z small, which is the very peak of the Compton profile). IA (the leading order of the expansion) is, however, quite good even for $a/k \simeq 1$.

We may note the presence of a/k and $(a/k)^2$ terms in the expansion equation (19), not just the term $(a/k)^4$ as Eisenberger and Platzman (1970) argue. [EP write this term as $(E_B/E_{p_f})^2$, where $E_B = a^2/(2m)$ is the K-shell binding energy and $E_p = p_f^2/2m$ is the

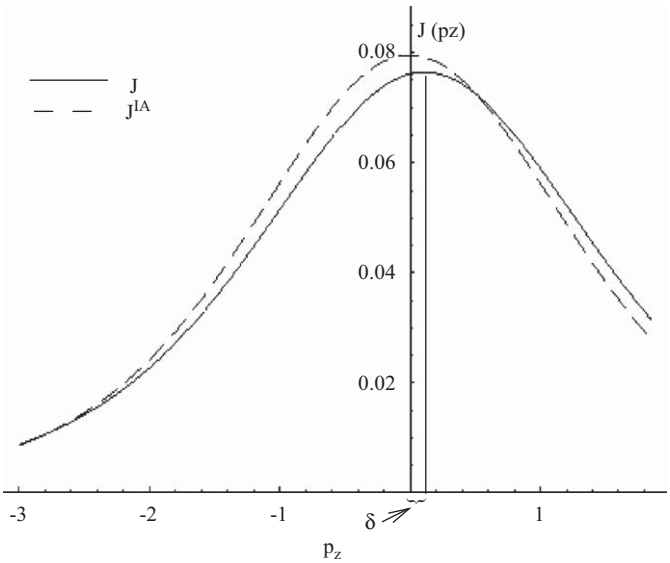

Fig. 4. Compton profile, as a function of p_z for fixed $a/k = 0.54$ ($a = mZ\alpha$), for a Be K-shell electron in a hydrogenic model. The dashed line shows the IA result, J^{IA}, and the full line shows the A^2 result. IA is good even for a/k of the order of unity, for the profile J. Note that the maximum of the exact Compton profile is shifted (by some amount δ) from the position of the maximum in IA (at $p_z = 0$).

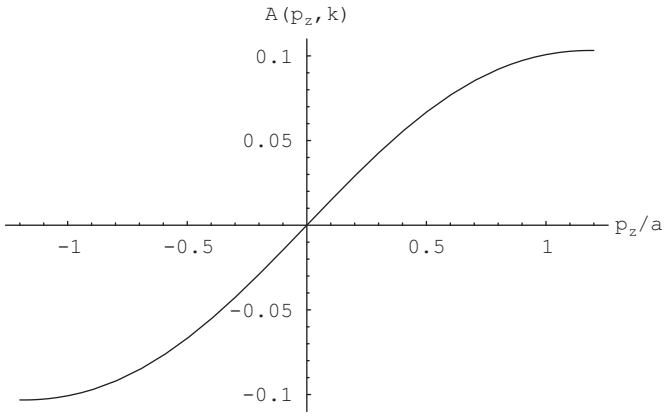

Fig. 5. Asymmetry $A(p_z,k)$, Eq. (20), as a function of p_z for the case shown in Fig. 4. $A(p_z,k)$ is largely just a shift. See Fig. 6 and text.

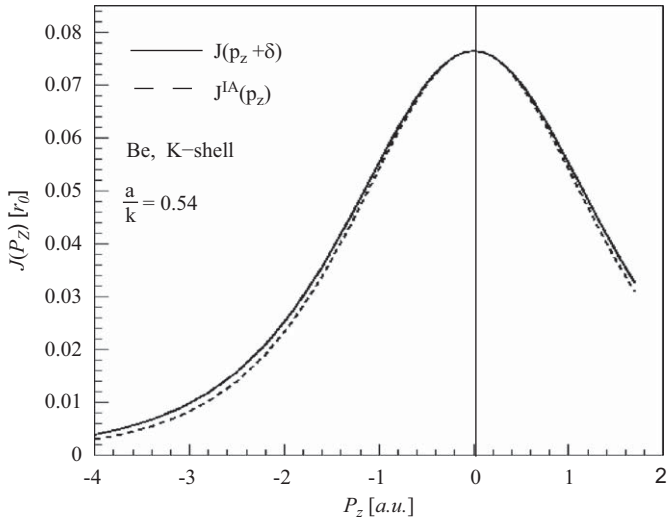

Fig. 6. The Compton profile of the Be K-shell from Fig. 4 ($a/k=0.54$), shifted to compare with a renormalized IA result (dashes). The results of IA are normalized (multiplying by 0.98) to have the same maximum as the exact result. Comparison of the A^2 Compton profile with the shifted (and normalized) IA profile (which is symmetric about the peak) shows that the true asymmetry of the profile is small.

outgoing electron kinetic energy. Since $p_f \simeq k$ this corresponds to $(a/k)^4$.] Despite the fact that a/k and $(a/k)^2$ terms are present, IA is in fact good even for $a/k \simeq 1$.

4.3. Validity of nonrelativistic IA for DDCS: asymmetry

While in IA the Compton profile is a symmetric function of p_z, in exact Compton profile this is not true. The positions of the peaks in IA and in A^2 approximation differ by some amount δ. The heights of the peaks are also different. This is illustrated in Fig. 4 using Compton profile for the Coulomb K-shell for $Z=4$. The presence of the linear term p_z/a in the expansion equation (19) of the exact Compton profile is the reason that the exact Compton profile shows an asymmetry $A(p_z,k)$, as conventionally defined (Huotari et al., 2001), around $p_z=0$, i.e.

$$A(p_z,k)=\frac{J(p_z,k)-J(-p_z,k)}{J(p_z=0,k)} \tag{20}$$

is nonzero for the exact profile. The asymmetry $A(p_z,k)$, which corresponds to the case illustrated in Fig. 4, is shown in Fig. 5.

However, we have found that this asymmetry $A(p_z,k)$ is largely just a shift δ, with normalization, even relativistically (except for high Z). A new definition of asymmetry was proposed by Chatterjee et al. (2007). The relative difference between a shifted Compton profile J (shifted by δ so that its maximum is at $p_z=0$) and the IA prediction J^{IA}, properly normalized to give the same peak value as J, can be partitioned into small symmetric S and antisymmetric A' parts

$$\frac{J(p_z+\delta,k)-NJ^{IA}(p_z))}{J(\delta,k)}=S(p_z,k)+A'(p_z,k). \tag{21}$$

The A' defined in this way is the true asymmetry of the Compton profile, while S is the main deviation from IA shape. Fig. 6 illustrates that the shifted J has very small asymmetry A'. In the case shown in Fig. 6, $S\lesssim 1\%$ and $A'\lesssim 0.05\%$ for $|p_z/a|\lesssim 1$.

4.4. Relativistic behavior

In the RIA of Ribberfors (1975), scattering from bound electrons is still viewed as scattering from a distribution of free electrons. As in nonrelativistic IA, this approach can be used to obtain RIA for both TDCS and DDCS. A revised description of deviations from IA in term of shift and normalization is also applicable at relativistic energies, except, however, for high Z K-shell Compton scattering (as demonstrated numerically). RIA

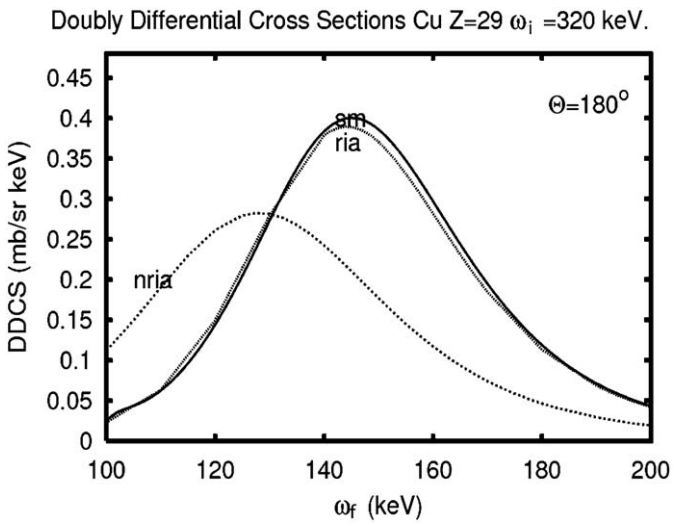

Fig. 7. DDCS, for scattering from the K-shell of Cu, $Z=29$, as a function of scattered photon energy. Shown are: the results of our S-matrix calculations (**sm**); relativistic IA (**ria**), nonrelativistic IA using nonrelativistic kinematics and p_z (**nria**).

(relativistic IA) is found adequate under the same conditions as IA, except in this one case (Chatterjee et al., 2007; Pratt et al., 2007).

Relativistically, it is not generally true that $d^2\sigma \propto J(p_z)$. However, further approximations allow one to write

$$\frac{d^2\sigma}{d\omega_f\, d\Omega_f}=K_F\times[J(p_z)+C(J(p_z)], \tag{22}$$

where p_z is now determined by relativistic kinematics, K_F is a relativistic kinematical factor (which is a function of ω_i, ω_f and θ), and Ribberfors argued that $C(J(p_z)$ is a very small correction at large angles, and also for low Z. The validity at large angles for large Z is now being questioned (LaJohn, 2009).

It is interesting to note that the Ribberfors approximate result [Eq. (22) neglecting C] can be obtained directly from nonrelativistic IA (LaJohn, 2009) providing that: (1) kinematics and the kinematical factor are described relativistically, (2) a relativistic

definition of the p_z is used (note that Ribberfors uses a different notation for our p_z), and (3) a relativistic charge density is used.

In Fig. 7 we compare a full S-matrix calculation with RIA in the peak region of the DDCS for a low Z Coulomb K-shell case at an incident energy of 320 keV. The RIA results agree very well with the S-matrix calculations while nonrelativistic IA (denoted by nria) completely fails. In Fig. 8 we give similar results for a high Z and somewhat higher energy (450 keV). In this case the infrared behavior (denoted with LET) is not completely separated from the peak region. The RIA result is in poor agreement with the S-matrix result. However, the sum of RIA result and LET result does quite well until approaching the center of the peak.

It is natural to ask whether further increase of incident photon energy improves the agreement between full S-matrix results and RIA results in the peak region. The answer is that corrections to RIA persist in the peak region for high Z even at ultrarelativistic energies, as follows from the study of Florescu and Pratt (2009). The corrections are scaling as Z (about 15% for $Z=92$). This is illustrated in Figs. 9 and 10. Contributions of the infrared rising terms (not included in RIA) on the low energy side are significant for large Z.

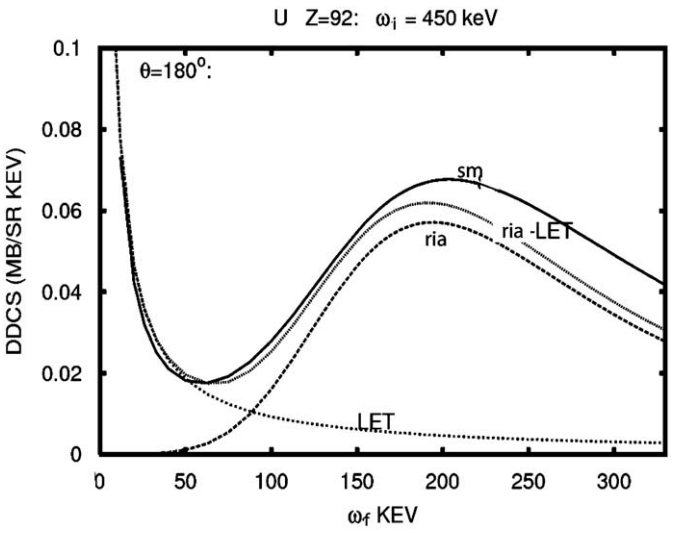

Fig. 8. DDCS as a function of scattered photon energy, for scattering of 450 keV photons from the K-shell of U, $Z=92$, into 180°. Shown are: the results of our S-matrix calculations (**sm**); relativistic IA (**ria**); the results (**LET**) obtained using the low energy theorem (Bergstrom et al., 1993), which predicts the infrared behavior [rise of the DDCS as $\omega_f \to 0$]; the sum of **LET** and **ria** results (**ria–LET**). The figure shows that the infrared behavior for high Z is not entirely separated from the peak region, which illustrates that the importance of the $\mathbf{p}\cdot\mathbf{A}$ term is large in this case, in which $a/k \lesssim 1$.

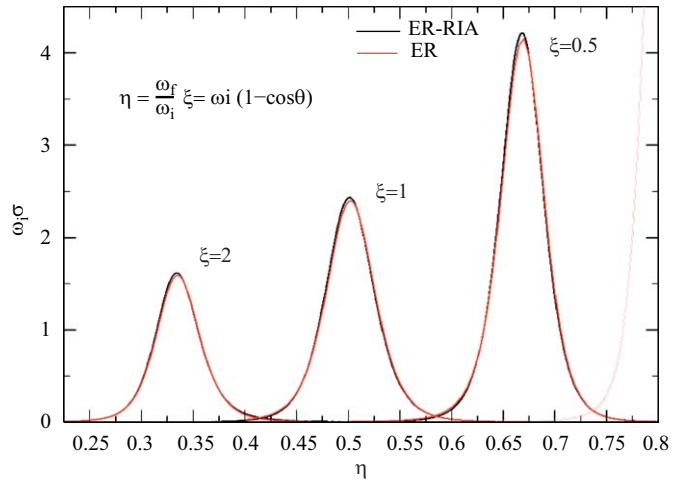

Fig. 9. $\omega_i \cdot \sigma$ as a function of the variable $\eta = \omega_f/\omega_i$ for various $\xi = \omega_i(1-\cos\theta)$, for $Z=29$. $Z\alpha$ corrections are small at ultrarelativistic limit.

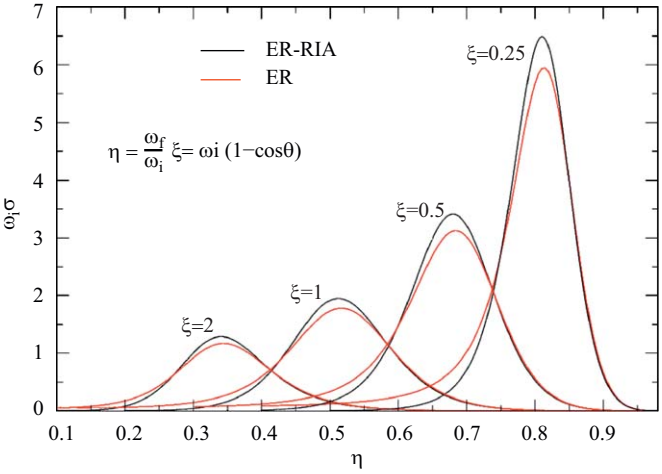

Fig. 10. $\omega_i \cdot \sigma$ as a function of the variable $\eta = \omega_f/\omega_i$ for various $\xi = \omega_i(1-\cos\theta)$, for $Z=82$. $Z\alpha$ corrections are about 12%.

5. Summary

We have discussed the development of the theory of Compton scattering, with particular attention to impulse approximation (IA). IA provides the most widely used description of Compton scattering in the peak region. IA gives a simple connection between DDCS and momentum distribution $\rho(\vec{p})$. Other approaches (S-matrix, A^2) provide a measure of the validity of IA, but are more complicated and have been restricted to IPA. IA can be applied to TDCS as well as DDCS, but for TDCS it is only valid at high energy. IA for DDCS is much better than for TDCS and also better than Eisenberger and Platzman (1970) estimated. The biggest correction to IA, asymmetry of the profile, is really a shift of the spectrum. In the relativistic region, $\vec{p}\cdot\vec{A}$ contributions overlap A^2 contributions and corrections to IA are large in the peak region for high Z. Corrections to relativistic IA persist in the peak region for high Z even at ultrarelativistic energies.

Acknowledgments

This work has been supported by NSF Grant nos. 0456499 and 0352483, by Croatian MZOS Grant no. 098-0982931-2875, by Indo-US collaborative project DST-NSF/RPO-138 and by Romanian Grant CEEX-D11-56-05.

References

Bergstrom, P.M., Pratt, R.H., 1997. Rad. Phys. Chem. 50, 3.
Bergstrom, P.M., Surić, T., Pisk, K., Pratt, R.H., 1993. Phys. Rev. A 48, 1134.
Bloch, B.J., Mendelsohn, L.B., 1974. Phys. Rev. A 9, 129.
Bloch, F., 1934. Phys. Rev. 46, 674.
Chatterjee, B.K., Roy, S.C., Surić, T., LaJohn, L.A., Pratt, R.H., 2007. Nucl. Instr. Methods A 580, 22.
Chew, G.F., 1950. Phys. Rev. 80, 196.
Chew, G.F., Wick, G.C., 1952. Phys. Rev. 85, 636.
Compton, A.H., 1923a. Phys. Rev. 21, 483.
Compton, A.H., 1923b. Phys. Rev. 22, 409.
Cooper, M., Leake, J.A., Weiss, R.J., 1965. Philos. Mag. 12, 797.
Cooper, M., 1985. Rep. Progr. Phys. 48, 415.

Costescu, A., Gavrila, M., 1973. Rev. Roum. Phys. 18, 493.
DuMond, J.W.M., 1929. Phys. Rev. 33, 643.
DuMond, J.W.M., 1933. Rev. Mod. Phys. 5, 1.
Eisenberger, P., Platzman, P.M., 1970. Phys. Rev. A 2, 415.
Fermi, E., 1936. Ric. Sci. 7, 13.
Florescu, V., Gavrila, M., 2003. Phys. Rev. A 68, 052709.
Florescu V., Pratt, R.H., 2009, submitted for publication.
Gummel, A., Lax, M., 1957. Ann. Phys. (N.Y.) 2, 28.
Gavrila, M., 1972. Phys. Rev. A 6, 1348.
Gavrila, M., Tugulea, M.N., 1975. Rev. Roum. Phys. 20, 209.
Gray, J.A., 1920. J. Franklin Inst. 190, 633.
Holm, P., Ribberfors, R., 1989. Phys. Rev. A 40, 6251.
Huotari, S., Hämäläinen, K., Manninen, S., Issolah, A., Marangolo, M., 2001. J. Phys. Chem. Solids 62, 2205.
Jauncey, G.E.M., 1925. Phys. Rev. 25, 314.
Kaliman, Z., Surić, T., Pisk, K., Pratt, R.H., 1998. Phys. Rev. A 57, 2683.
Kane, P.P., 1992. Phys. Rep. 218, 67.
Klein, O., Nishina, Y., 1929. Z. Phys. 52, 853.
LaJohn, L.A., 2009, submitted for publication.
Platzman, P.M., Tzoar, N., 1965. Phys. Rev. 139, A410.
Prasad, P.N., Basavaraju, G., Kane, P.P., 1977. Phys. Rev. A 15, 1984.
Pratt, R.H., LaJohn, L., Surić, T., Chatterjee, B.K., Roy, S.C., 2007. Nucl. Instr. Methods B 261, 175.
Ribberfors, R., 1975. Phys. Rev. B 12, 2067.
Schnaidt, F., 1934. Ann. Phys. (Leipzig) 21, 89.
Schumacher, M., Smend, F., Borchert, I., 1975. J. Phys. B 8, 1428.
Surić, T., Bergstrom, P.M., Pisk, K., Pratt, R.H., 1991. Phys. Rev. Lett. 67, 189.
Surić, T., 1992. Nucl. Instr. Methods A 314, 240.
Tavard, C., Dalcappello, M.C., Gasser, F., Dalcappello, C., 1983. Phys. Rev. A 27, 199.
Wentzel, G., 1927. Z. Phys. 43, 1.
Wick, G.C., 1954. Phys. Rev. 94, 1228.
Whittingham, I.B., 1971. J. Phys. A 4, 21.
Wittwer, L.A., 1972. Lawrence Radiation Laboratory Report No. UCRL-51268, Livermore, CA, unpublished.